Thermal performance of thermo-active CFA piles

Fleur Loveridge, MSc, PhD, FGS, CGeol, CEng, MICE

Royal Academy of Engineering Research Fellow and Lecturer in Geomechanics, Faculty of Engineering and the Environment, University of Southampton, Southampton, UK

Francesco Cecinato, MSc, PhD

Lecturer in Geomechanics, Department of Civil, Environmental and Mechanical Engineering, University of Trento, Trento, Italy

Corresponding author: Francesco Cecinato, Department of Civil, Environmental and Mechanical Engineering, University of Trento, Via Mesiano 77, 38123 Trento, Italy, email: francesco.cecinato@unitn.it

Abstract

Foundation piles are being increasingly equipped with heat exchangers to efficiently harvest shallow geothermal energy. For buildings in urban areas continuous flight auger (CFA) piles are common due to their speed, cost efficiency and low noise levels. To construct a thermo-active CFA pile usually requires separate central installation of the heat exchanger. However the energy performance of this type of pile has not been investigated systematically, with most studies focused on rotary piles where the heat exchanger is attached to the reinforcing cage. In this work, insights are provided about the main influences on the energy efficiency of thermo-active CFA piles, with a focus on the implications of using CFA construction techniques rather than rotary boring. An innovative 3D numerical model, able to capture the different aspects of transient heat transfer, is employed together with analytical methods to evaluate the transient and steady-state behaviour of energy piles in a number of design situations. Attention is given to understanding the role of possible pipe to pipe interaction, which cannot be systematically investigated with standard methods. Finally, practical guidelines on the optimal choice of design parameters to maximise the energy efficiency of CFA piles, without altering the geotechnical arrangements, are provided.

Keywords

Energy Geotechnics; Piles & piling; Thermal effects.

List of notation

T	temperature
t	time
$\mathbf{x}$	spatial coordinates vector
ρ	density
$\dot{m}$	mass flow rate
c_p	specific heat capacity
λ	thermal conductivity
Q	exchanged power
q	exchanged power per unit length
E_{tot}	total exchanged energy
v	fluid velocity
n_p	number of pipes
L	pile length
D	diameter
R	thermal resistance
c	distance between pipe and pile edges
s	centre-to-centre pipe shank spacing

Subscripts

f	fluid
c	concrete
g	ground
m	*model*
s	steel, solid
in	inlet
out	outlet

2 two-dimensional

3 three-dimensional

1 Introduction

Every year the floor area of the European building stock increases by approximately one percent, resulting in additional energy consumption of over 4.5 million tonnes of oil equivalent (BPIE, 2011). At the same time, the European Union has ambitious carbon dioxide emissions reduction targets (Council Direction, 2009) which are in conflict with such increases in demand. One approach for reducing both energy and carbon dioxide emissions from buildings is to adopt shallow ground energy systems, where ground heat exchangers are combined with a heat pump to improve energy efficiency, potentially reducing demand by around 75%, depending on the system coefficient of performance.

Further financial and embedded carbon economies can potentially be made by using the foundations piles of a building to host the heat exchanger part of the ground energy system, so called thermo-active piles or energy piles. This innovation was pioneered in the 1980's in Austria and Germany (Brandl, 2006). However, progress towards more global adoption of thermo-active piles and other geo-structures has only taken place more recently (e.g. Barla & Perino, 2014, Laloui & Di Donna, 2012). This has triggered a renewed interest in thermo-active pile research and for the first time there has also been a focus on maximising the energy efficiency of these systems (Cecinato & Loveridge, 2015, Bozis et al, 2011, Wood et al, 2010, Gao et al, 2008).

For piles to become thermo-active, polyethylene pipes must be embedded within the pile concrete to allow the heat transfer from the ground to the energy system to occur via a circulating fluid. However, there are a number of different ways in which foundations piles can be equipped with pipes, and these depend largely on the construction method of the pile itself. In most cases, rotary bored piles are the most common type of pile used as heat exchangers. However, particularly in the UK, continuous flight auger (CFA) piles are increasingly being used given their prevalence in the building development sector, for example see Loveridge & Powrie, 2013a. This paper will examine the advantages and disadvantages of the use of CFA piles for thermo-active foundations. While the main focus is energy efficiency implications, the following section will also discuss the construction considerations.

2 Construction Techniques

The use of CFA piles has grown in recent years owing to their many advantages, but not least due to their speed (and therefore reduced cost) of installation compared with rotary bored piles. In addition, CFA piles are quiet to install and produce low levels of vibrations, making them suitable for city centre sites where new building development may be concentrated. They are, however, not suitable for all ground conditions and are practically limited in size and depth due to plant capabilities. A review of situations where CFA piles will be economic and those for which they are unsuitable is given by Brown (2005).

When it comes to thermo-active piles one important difference in the construction method effects how the heat exchange pipes are introduced into the concrete. In the construction of traditional rotary bored piles the steel reinforcing cage is hung from the pile casing while concrete is placed inside the pile bore, usually via a tremie pipe. In CFA piling, the concrete is pumped into the pile bore via the hollow stem of the auger, which is then withdrawn as concreting progresses. As a result the steel reinforcing cage must be plunged separately into the wet concrete after the auger has been withdrawn.

The most practical and economic way to introduce heat transfer pipes to the foundation is via attachment of the pipe U-loops to the reinforcing cage. Installation of the pipe loops over the full depth of the pile is essential as the heat transfer length is a key factor in the thermal efficiency of piles used as heat exchangers (Cecinato & Loveridge, 2015). However, for most building development projects (unless the piles are required to carry tension), the steel reinforcement is not required over the full depth of the pile. Consequently, depending on the construction method of the pile, additional specific measures are required to ensure the pipes reach the full depth of the pile bore.

For rotary bored piles where the steel cage is installed ahead of the concrete, it is possible to attach full length pipe loops to the reinforcement and allow these to hang beneath the cage during concreting. In this way the pipes may reach the full depth of the pile even if the cage does not. Sometimes additional weight maybe required to be attached to the pipes at the base to prevent buoyancy within the concrete due to the presence of fluid within the pipes, but otherwise the combined reinforcement cage and pipe installation process is straightforward. If the steel cage is constructed in one piece it is then possible to attach the pipes during pre-fabrication offsite. This means that there is no impact on the piling programme during construction. If the piles are of sufficient depth that the steel cages require splicing then the pipes will instead need to be attached to the cage sections during their installation. Nevertheless a full depth pipe installation based on attachment to the reinforcement cage is still easily accomplished.

For CFA piles, however, a different approach must be adopted. Because the steel reinforcing cage is plunged into the wet concrete, it is only possible to insert pipes with the steel cage if the pipes are limited to the length of the cage. Because the reinforcing cage is rarely full depth for a building foundation, an alternative approach to installation of the pipes is usually adopted to maximise the available heat transfer length and hence energy efficiency. To permit a full depth installation the pipes must be installed separately following insertion of the pile cage into the concrete. Typically the pipes are attached to an additional steel bar for weight and rigidity and then plunged into the centre of the pile. This additional operation during construction means that there can be some supplementary programme time required for converting CFA piles to thermo-active piles. Additional construction considerations may also arise including the need for the concrete to remain workable until the loops are installed (more problematic in certain ground conditions) and whether a handling crane will be available to lift the loops (Amis et al, 2015).

Owing to these different construction approaches, rotary bored piles tend to have their pipes spaced apart around the steel cage (Figure 1a), which is typically only 50mm to 75mm from the ground. Typical pipe spacings are between 250mm and 300mm (Loveridge & Powrie, 2013b). CFA piles on

the other hand, will more typically have their pipes installed closer together in the centre of the pile (Figure 1b) and pipe spacings rarely exceed 60mm. Practically no more than four pipes (two U-loops) are usually installed in the centre of CFA piles, while many more pipes may be placed in rotary bored piles depending on their diameter.

3 Thermal Performance Assessment

3.1 Background

Recently a systematic assessment of the thermal efficiency of rotary bored piles was carried out based on numerical simulation (Cecinato & Loveridge, 2015). This assessment ranked a number of key design parameters in the order of their impact on the thermal performance of the pile. The most important parameter was found to be the number of pipes installed in the pile cross section, followed by the length of the pile. The latter parameter highlights the importance of ensuring the pipe loops are installed over the full depth of the pile since the piled foundation will rarely be extended in depth to accommodate greater energy availability. Following the pile depth, its thermal conductivity and the diameter of the cross section were also found to be important. Of these four parameters the number of pipes installed is the most straightforward to engineer for thermal performance, followed by the concrete conductivity. Although the latter will also be influenced by the economics of available aggregate sources, and often closer sources may be chosen over those which are more thermally advantageous but require greater transport distances. Like the pile length, its diameter is unlikely to be adjusted only to satisfy the thermal design.

Based on the results of the study undertaken for rotary bored piles it is likely that the number of pipes installed and the concrete conductivity would influence the efficiency of CFA piles. Additionally CFA piles would be expected to be less energy efficient than rotary piles for two reasons. First, the pipes installed will always be closer together (Figure 1) and second, practically fewer pipes may be installed within a CFA pile. Additionally there have been concerns that close proximity of the pipes in CFA piles, as well as their installation with a high thermal conductivity material (the steel bar), would make this arrangement vulnerable to pipe to pipe interactions. Adverse pipe to pipe interactions have been studied for borehole heat exchangers (e.g. Muraya et al, 1996, Lamarche et al, 2010), resulting in the common practice of using spacers between the two shanks of borehole U-loops. However, for the case of thermo-active piles, no assessment of the potential for pipe to pipe interactions has been made, and the thermal performance of CFA more generally has not previously been quantified.

3.2 Numerical Implementation

3.2.1 Model description

The model reproduces the three main heat transfer mechanisms taking place in thermo-active structures, namely thermal convection between the heat transfer fluid and the pipe wall, thermal conduction in the concrete, and thermal conduction in the ground.

The convection-diffusion equation that applies to the heat exchanger fluid is

$$\dot{m} c_{pf} \nabla T = h \Delta T \tag{1}$$

where c_{pf} is the fluid specific heat capacity, $\dot{m} = \rho v A$, the mass flow rate, A is the pipe cross-sectional area, v is the fluid velocity, ρ is the fluid density, *h* is the 'film' (or convective heat transfer) coefficient, and $\Delta T = \left(T_s - T_f \right)$, the temperature difference between the solid interface (pipe wall) and the fluid.

It is assumed that (i) convection due to fluid flow occurs as a quasi-static phenomenon, and (ii) conductive heat transfer along the flow direction can be neglected compared to both the radial heat transfer at the fluid/pipe wall interface and the convective transfer. In addition, the contribution of friction heat dissipated by viscous shear is neglected (cf. Cecinato and Loveridge 2015). These simplifications have been shown to be appropriate with the modelling approach validated against field data and analytical solutions, both for borehole heat exchangers (Choi et al. 2011) and rotary bored piles (Cecinato and Loveridge 2015).

The heat transfer through the pipe wall, concrete and the ground is governed by standard transient heat conduction, as

$$\rho_s c_{ps} \dot{T} = \nabla \left(\lambda_s \nabla T \right) \tag{2}$$

where ρ_s, c_{ps} and λ_s are respectively the density, specific heat capacity and thermal conductivity of the considered solid material, and $\dot{T}$ is the temperature time rate.

The transient heat convection-diffusion problem was solved employing the software ABAQUS to integrate 3D transient conduction through the solids, complemented by writing bespoke user subroutines to model the convective heat transfer at the fluid/solid interface and the temperature changes in the fluid along the pipe. Each solid material (soil, concrete and steel) was defined by specifying its density, specific heat and conductivity. At each time step, alongside the standard ABAQUS calculation of heat diffusion in the concrete/ground, the necessary convection computations were performed in a semi-coupled way involving (i) the calculation via subroutine *FILM*, at each pipe segment, of the radial heat flux; (ii) the calculation via subroutine *URDFIL*, at each pipe node, of the fluid temperature change. Further details of the ABAQUS model can be found in Cecinato and Loveridge (2015).

The 3D FE mesh was created manually in an axisymmetric fashion using 6-node linear triangular prism and 8-node linear brick diffusive heat transfer elements (Figure 2). The size of the domain (5.5 m of diameter and 29 m of depth) was chosen by numerical experimentation to be much larger than the area actually affected by heat transfer. It should be observed that the approach outlined implies the schematisation of the pipes within the FE mesh as lines of nodes, where the heat exchange resulting from convection-diffusion in the pipes is concentrated. The 3D nature of the pipes (i.e. the relevant diameter, in addition to length) is properly accounted for via the user subroutines, by multiplying the heat flux corresponding to each pipe node by the corresponding lateral surface area of each pipe segment. As a consequence, each pipe node in the 3D mesh lies in the barycentre of a

pipe segment. Correspondingly, if a 2D cross-section of the domain is considered, each node lies in the centre of the circular pipe cross-section (Figure 2).

3.2.2 Simulation settings

A single CFA energy pile is represented in the mesh. Whenever two pipes (a single U-loop) are installed significant calculation time saving is made by exploiting the symmetry of the problem, since only half of the domain is considered. However, the complete domain must be considered whenever two or more U-loops connected in series are present.

As boundary conditions, the inlet fluid temperature is prescribed with a constant inlet temperature of 20°C, after a short initial ramp lasting 5' to avoid possible numerical problems due to the abrupt temperature change. As initial (undisturbed) ground temperature a value of 12 °C (averagely representative of central Europe) was chosen. The initial ground temperature is also taken as the farfield boundary conditions. A total simulation time of 4 days was set for all analyses, which could be typical of a thermal response test on a large diameter pile, and short enough to save computational time.

The key outputs from the simulations are the outlet temperature history $T_{out}(t)$ (i.e. the temperature of the fluid as it exits the pile, at ground level), the fluid temperature history at every node constituting the pipes $T_f(\mathbf{x},t)$, the pipe and pile wall temperature histories $T_{pipe}(\mathbf{x},t)$ and $T_{pile}(\mathbf{x},t)$, where $\mathbf{x}$ is the spatial coordinates vector and t time.

The energetic efficiency can be assessed by considering at the total exchanged energy in a given time. The total exchanged power Q can be calculated from each simulation as

$$Q(t) = \dot{m} c_{pf} \left[T_{in}(t) - T_{out}(t) \right] \tag{3}$$

where $T_{in}(t)$ the design inlet temperature history. The output variable representing energy exchanged can be then computed as

$$E_{tot} = \int_0^{t_f} Q(t)\, dt \tag{4}$$

where t_f = 4 days, the total simulation time.

3.3 Cases Considered

3.3.1 Sensitivity Analysis

A sensitivity study was performed with the above calculation hypotheses, by carrying out a number of simulations while varying the parameters that are potentially easier to engineer for CFA piles, keeping constant at typical values the model parameters that do not exhibit a high variability or

cannot be easily engineered. To focus on the features that are peculiar of CFA piles, and in light of the existing knowledge on the sensitivity of rotary piles to a large parameter set (Cecinato and Loveridge 2015), for a first CFA parametric study the decision was made to vary the number of pipes, n_p, and the fluid velocity, v, only. We consider n_p to take two possible values, n_p=2 (a single U-loop) and n_p=4 (a double U-loop). Practically, due to limited space availability around the steel bar used in CFA construction, greater numbers of pipes are not usually installed. All double U-pipe settings consider pipes connected in series, as this is the most common design option in practice. The fluid velocity is a relatively free design parameter that can be considered to vary within a wider range of values, $0.2 \le v \le 1.2$ m/s. To systematically and efficiently investigate the variable parameter space, a total of eight simulations were performed, as summarised in Table 1.

Among the parameters that are kept constant, the pile length L and diameter D_{pile} are set to 25 m and 900 mm respectively; these are at the upper bound for typical CFA piles, but provide convenient sizes for comparison to rotary construction. The concrete and the ground are assumed to be fully water-saturated and to take typical values (Table 2). The pipes are considered to be attached to a central steel bar with diameter $D_{bar} = 40$ mm and are assumed to take a symmetric arrangement (Figure 2). All fixed model parameters are summarised in Table 2.

3.3.2 Comparison to Rotary Bored Piles

For proper comparison with rotary pile situations, three extra simulations (called run 3rot, run 5rot and run 7rot; Table 3) were carried out keeping the same settings of run 3, run 5 and run 7 (Table 1), but changing the pipe position to achieve a concrete cover of $c = 75$ mm, as is typical of rotary bored piles where pipes are attached to the reinforcement cage (Figure 3). These simulations investigate the effect of increased pipe shank spacing, s, in both single and double U-loop cases and with different fluid velocity scenarios.

The numerical model was also used to examine pipes installed with an intermediate shank spacing between CFA and rotary piles (called run 7int; Table 3). While such an arrangement is unlikely to ever be constructed in practice, these simulations were conducted to aid interpretation of the other results.

3.3.3 Pipe Positioning

While the analyses described in 3.3.1 consider a centrally (and axially) symmetric arrangement for the pipes, the situation exists in practice, in the absence of spacers, when the pipes are embedded into the pile concrete in a bunched fashion, so that they are not regularly distributed around the steel bar (Figure 4a). Bringing the pipes closer to each other compared to a symmetric arrangement, the question may arise whether this will have an impact on the overall energy performance. Thus, a further simulation was carried out (called run 7_unsym; Table 3) with the same settings as in run 7, but applying a worst case unsymmetrical pipe arrangement (Figure 4b).

3.3.4 The Impact of the Steel Bar

Finally, the sensitivity of results to the presence of the central steel bar, or the variation in its thermal conductivity was investigated by running two simulations, called run 3_Lc and run 3_Lh (Table 3). The same settings as in run 3 were adopted, except for the conductivity of the central bar

material, that was set to 3 W/mK in the former case (i.e. considering the same conductivity as concrete), and to 73 W/mK in the latter case (i.e. considering the bar to be composed of an extremely conductive steel).

4 Results

4.1 Energy Performance

4.1.1 Results of Sensitivity Study

In Figure 5 the results of the numerical sensitivity analysis described in Section 3.3.1 are reported, in terms of a) outlet fluid temperature evolution and b) evolution of exchanged power per meter depth of the pile. It can be observed that the largest temperature change is achieved when the fluid velocity is smallest (run5 and run1), however by virtue of Equation (3), more thermal power is exchanged at larger mass flowrates. Figure 5b shows that the number of pipes also increases the exchanged power, hence in principle the efficiency of the geothermal structure. To better quantify the energy performance, in Figure 6 the total energy exchange E_{tot} (Equation (4)) for each simulation is shown. It emerges that that the energy efficiency of CFA piles is an increasing function of both fluid velocity and of the number of pipes, the latter being more influential in absolute terms. It is also clear that the energetic benefit of increasing the velocity is weaker in the upper range of typical velocities. The biggest increase in energy exchanged is from *v=0.2* m/s to *v=0.4* m/s. This corresponds to an increase in Reynolds number from 4,900 to 9,800, i.e. the exit from the transient zone into fully turbulent flow. In other words, as already observed for rotary bored piles by Cecinato and Loveridge (2015), provided that the fluid velocity is large enough to ensure turbulent flow, increasing it further would only have a secondary impact in the energy efficiency. Additionally, for any operational system it must also be considered that increasing the flow rate will require a corresponding increase in the pumping energy which will have a detrimental effect on the overall system performance. These two factors will need to be balanced during system design.

4.1.2 Comparison to Rotary Bored Piles

Figure 7 shows the comparison between CFA and rotary bored piles with the same properties, but with different shank spacing. Both the exchanged power and outlet fluid temperature are presented for each simulation. In all cases, the rotary arrangements show a larger temperature change, and a corresponding larger exchanged power, implying a larger energy exchange in the considered time window. To corroborate this outcome, in Figure 8 the total energy exchanged is shown for all cases. It can be observed that the energetic improvement when switching between the CFA and the rotary configuration is substantial, increasing by up to a factor of two in the four pipe case (run 7).

4.1.3 Effect of Central Bar and Pipe Arrangements

By comparing the output of simulations run3 (standard CFA settings), run3_Lc (central bar as conductive as concrete), and run3_Lh (central bar made of highly conductive steel) a negligible difference is observed, both in terms of exchanged power and of total energy. Variation between the three simulations is within 1%. Hence, it can be concluded that the presence of the steel bar does not affect the pile thermal performance.

On the other hand, different pipe arrangements appear to have a major impact on the energy performance. As can be seen in Figure 9a, a significant decrease of exchanged power is obtained with run7 settings switching from a symmetrical CFA pipe arrangement to an unsymmetrical CFA arrangement (run7_unsym). This could be due to pipe to pipe interactions, in that part of the heat may be exchanged between adjacent pipes, not contributing to outwards heat diffusion (the potential for pipe to pipe interactions is further discussed in Section 4.2). Keeping the symmetrical pipe configuration and increasing the shank spacing, from a CFA situation (run7) through an intermediate case (run7_interm), to a rotary configuration (run7rot), the exchanged power substantially increases. This is also reflected by the evolution of average pile wall temperature over time, shown in Figure 9b for run7 at different pipe configurations. Larger pile wall temperature changes correspond to larger overall exchanged energy (Figure 9c).

As a further example of the model simulation capabilities, the distribution of temperature around the pile cross section at the end of the simulation time are shown in Figure 10. Typical temperature contours are shown at pile mid-depth (z=12.5 m), for a 2-pipe arrangement (run 3) in both CFA (Figure 10a) and rotary (Figure 10b) configuration, and for a 4-pipe arrangement (run7) in both symmetrical CFA (Figure 10c) and unsymmetrical CFA (Figure 10d) configuration. It can be noticed that less symmetrical cross-sectional temperature distributions occur in the 2-pipe rotary case and in the unsymmetrical CFA arrangement. It is also observed that in the rotary case, when shank spacing is significantly larger, the ground temperature increase is also larger, all other things being equal, due to the proximity of the pipes to the ground, and to the wide separation between the two pipes which keeps pipe to pipe interactions to a minimum.

4.2 The Potential for Pipe to Pipe Interactions

The potential for pipe to pipe interactions in CFA piles has been assessed by considering the numerically calculated concrete thermal resistance of the pile in comparison with that determined from analytical solutions. The concrete resistance (R_c) is a steady state parameter that is defined as:

$$R_c = \left(\overline{T}_{pipe} - \overline{T}_{pile}\right) \Big/ q \tag{5}$$

Where $\overline{T}_{pipe}$ is the average temperature on the outside of the pipes, $\overline{T}_{pile}$ is the average pile wall temperature and q is the exchanged power per metre depth of the pile. When defined from the outputs of the numerical model an additional subscript “m” will be used to distinguish the value from analytically derived thermal resistance.

Analytically, the concrete resistance can be determined in two dimensions (R_{c2}) using the line source method (Hellstrom, 1991). This approach is easy to implement for a single U-loop and has been complemented by using the simplified method of Loveridge & Powrie (2014) for the case of two U-loops. However, to include the effects of pipe to pipe interactions a pseudo-three dimensional version (R_{c3}) must be determined (Hellstrom, 1991), which is only readily applicable to the single U-loop case. Both the line source method and the calculation of R_{c3} according to Hellstrom have been validated by Lamarche et al (2010) for borehole heat exchangers using numerical simulation. Full equations for the analytical calculation of the concrete resistance are given in Appendix A.

To make appropriate comparisons between the numerically and analytically determined pile resistances it is first important to determine whether the concrete in the piles has approached a steady state. The concrete resistance from the model (R_{cm}) was calculated dynamically over the simulation time, examples of which are plotted in Figure 11. It can be seen that while the rotary piles reach steady state more rapidly, a steady state is still approached for the case of the CFA piles by the end of the simulation. By the end of the four day period the rate of change of pile thermal resistance was a maximum of 0.004 mK/W per day.

R_{cm}, determined at the end of the four day simulations, is compared with the analytical calculations in Figure 12. Considering first runs 1, 2, 3 and 4 with only a single U-loop installed it can be seen that the numerically determined R_c is larger than the analytical values in all cases. The two dimensional and three dimensional resistances are virtually equal for runs 3 and 4 with the highest flow rates, while for runs 1 and 2 the three dimensional resistance is slightly higher. Hence, based on the analytical calculations, pipe to pipe interactions seem to have a small impact even at lower flow rates and to be negligible at higher flow rates. However, the significantly higher values of numerically derived resistance could also suggest pipe to pipe interactions are occurring to a significant degree in all four cases. A similar result is seen for the four pipe CFA piles, although it has not be possible to determine R_{c3} in this case.

The discrepancy between the numerical concrete resistance and the analytical 3D resistance can potentially be explained by two options. First, as the analytical resistance is only pseudo-3D it is possible that the fully three dimensional numerical simulation is providing a better indication of the true extent of pipe to pipe interactions for CFA piles. This point of view is supported by considering the resistances determined for the rotary simulations. Here, where pipe to pipe interactions are not expected due to the larger shank spacing, the numerical and analytical resistances are much closer together (Figure 12). The case of the intermediate shank spacing (run 7int), half way between a rotary and a CFA arrangement, also shows similar results between the analytical and numerical calculations.

Alternatively, since the numerical model used does contain a simplification of the pipe problem (see Section 3.2.1), it is possible that the analytical solutions provide a better estimate of the degree of pipe to pipe interactions. If this is the case, then the numerical simplification only becomes of significance when the pipes are close together as is the case for the CFA analyses. Other researchers have used similar one-dimensional representations of pipes in the simulation of ground heat exchangers (e.g. Ozodogru et al, 2014, Signorelli et al, 2007). However, none of these models have been validated in terms of either field data or resistance calculation. Rees & He (2013) modelled borehole heat exchangers using a single layer of cells to represent the fluid. With this approach they found some short-term transient errors (up to 10%), but that the prediction of steady state resistance compared well with two dimensional analytical calculations, including for shank spacings closer than those considered for the CFA piles in this study. This may suggest that insignificant pipe to pipe interactions were occurring in their study. Therefore, the study of Rees & He (2013) lends some support to a possible over estimation of pipe to pipe interactions by the simulations for CFA piles presented above. On the other hand, the numerical model presented can be considered to

capture reasonably the dependency of resistance on different pipe arrangements (rotary, intermediate shank spacing, CFA and unsymmetrical CFA), as can be seen from the different arrangements for run 7 shown in Figure 12.

5 Discussion

This paper has presented the results from a range of simulations covering a number of different arrangements of CFA and rotary bored thermo-active piles. It is clear that the arrangement of pipes that results from the CFA construction process is less favourable in terms of energy performance than the same pile geometry constructed by rotary boring. Over four days the difference in energy exchanged may approach a factor of two, being represented by a reduction in concrete thermal resistance from 0.15 to 0.19 mK/W for CFA piles to 0.04 to 0.08 mK/W for rotary piles. This seeming disadvantage of CFA piles must be balanced against their speed of installation, low cost and reduced noise and vibration characteristics. These construction advantages for CFA piles in many urban sites tend to outweigh requirements for small amounts of additional programme time and the reduced energy efficiency of thermo-active CFA piles compared with traditional rotary bored piles. Consequently, it is unlikely that the inclusion of the pipe loops would influence the choice of construction method.

Instead, given a construction decision to install CFA piles rather than rotary bored piles, it is important to consider how to maximise the potential for energy performance when converting the piles to become thermo-active. Here, in line with other studies, analysis suggests that maximising the number of pipes and maintaining turbulence in the fluid will both contribute to improving energy output. Investigation of the presence of the steel bar, used to permit installation of the pipes in the concrete, showed that this high conductivity material does not have a significant effect on the energy exchanged. However, our analysis is showing for the first time the detrimental effects of allowing the U-loops to bunch together on the steel bar. This occurrence is common in construction and was seen to increase the concrete resistance of the pile by around one third for the case considered in this study. Such unnecessary effects could be removed by the use of spacers around the steel bar. This technique has been used successfully in test piles (Brettmann et al, 2010) and could be applied on a more routine basis.

CFA piles also offer another advantage compared to rotary bored piles that results directly from their increased thermal resistance. The resulting larger temperature difference between the heat transfer fluid and the ground means that the range of temperature change experienced by the ground and the ground-pile interface is reduced in CFA piles. This can be observed, for example, in Figure 9b (by comparing the curves representing the average pile wall temperature for the CFA and rotary cases) and has positive knock on effects for the geotechnical design which must consider whether any detrimental change in soil or interface properties may result from these temperature changes. Additionally, a larger volume of concrete between the pipes and the ground provides a buffer to the most extreme temperatures which the fluid may experience. These extreme temperature are often short lived and the concrete buffer may permit lower temperature limits to be set for the fluid without the risk of sub-zero temperatures reaching the ground. Such wider temperature limits will have a positive impact on the overall energy performance of the ground energy system.

One potential disadvantage for thermo-active CFA piles has been the concern that the potential for pipe to pipe interactions may lead to an increase in thermal resistance and hence a decrease in energy performance. The analysis carried out in this study tentatively suggests that there may be an increase in resistance (by up to 0.05mK/W or +25%) for CFA piles due to this mechanism. However, there remains a discrepancy between this result and calculations made by analytical methods which suggest only a small effect (maximum 6% increase in concrete thermal resistance) from pipe to pipe interactions and only at low flow velocities. Both approaches contain simplifications and it is not clear at present which approach is most appropriate. It would be beneficial to validate both approaches against thermo-active pile field data for CFA installations and also benchmark simulations containing a full representation of the heat transfer fluid. Nonetheless the results presented in this study are conservative and the discrepancies in resistance are small compared to the bigger differences (>0.1 mk/W) between CFA piles and rotary bored piles.

6 Conclusions

The following conclusions are presented from this study:

1. Thermo-active CFA piles will be less efficient than rotary piles on a like for like basis with equal numbers of pipes.
2. Rotary bored piles also offer the opportunity to install more pipes in the cross section, further increasing opportunities for maximising energy efficiency.
3. CFA piles are substantially cheaper than rotary bored piles to construct. However, some additional construction tasks are required to convert CFA piles to thermo-active structures, whereas this is not necessarily the case for rotary bored piles.
4. CFA piles are in common use for urban building developments. If converting to thermo-active piles then four pipes should be used instead of two, and care should be taken to ensure turbulence is maintained within the fluid.
5. The current practice of installing the heat transfer pipes with a steel bar for CFA piles does not appear to be detrimental to thermal performance. However, performance would be improved by adding the use of spacers to prevent bunching of the pipes on one side of the bar.
6. One additional potential advantage of CFA piles is that as the pipes are further from the pile edge, the soil-pile interface will experience a reduced temperature change compared with a rotary bored pile. This means that any influence on the geotechnical design will be reduced.

Acknowledgements

The first author is funded by the Royal Academy of Engineering under their Research Fellow scheme.

The second author acknowledges financial support from European Union FP7 project under contract number PIAPP-GA-2013-609758-HOTBRICKS.

Appendix A: Calculation of the Concrete Resistance

The two-dimensional pile concrete resistance is given by (Hellstrom, 1991):

$$R_{c2} = \frac{1}{4\pi\lambda_c}\left[\ln\left(\frac{D_{pile}}{D_{pipe}}\right) + \ln\left(\frac{D_{pile}}{2s}\right) + \sigma\ln\left(\frac{\left(D_{pile}/s\right)^4}{\left(D_{pile}/s\right)^4 - 1}\right)\right] \quad \text{(A1)}$$

The pseudo-three dimensional resistance is given by (Hellstrom, 1991):

$$R_{c3} = R_{c2}\eta\coth\left(\eta\right) \quad \text{(A2)}$$

where

$$\eta = \frac{L}{\dot{m}c_p\sqrt{R_{c2}R_a}} \quad \text{(A3)}$$

and R_a is the internal resistance, with

$$R_a = \frac{1}{\pi\lambda_c}\ln\left(\frac{2A_1\left(A_2^2+1\right)^\sigma}{A_2\left(A_2^2-1\right)^\sigma}\right) \quad \text{(A4)}$$

with $A_1 = D_{pile}/D_{pipe}$, $A_2 = D_{pile}/s$ and $\sigma = \left(\lambda_c - \lambda_g\right)/\left(\lambda_c + \lambda_g\right)$.

In the above expressions λ_g and λ_c and the thermal conductivity of the ground and the concrete respectively, D_{pile} is the outer diameter of the heat transfer pipes, D_{pile} is the diameter of the pile and s is the pipe centre to centre shank spacing.

References

Amis, T., McCartney, J. S., Loveridge, F., Olgun, C. G., Bruce, M. E. & Murphy, K. (2014) Identifying Best Practice, Installation, Laboratory Testing, and Field Testing, *DFI Journal*, 8 (2), 74-83.

Banks, D. (2012) An introduction to thermogeology: ground source heating and cooling, 2nd Edition, Wiley-Blackwell, Chichester, UK.

Barla M. & Perino A. (2014) Energy from geo-structures: a topic of growing interest, Env. Geotech. 2(1), 3-7.

BPIE (2011) Europe's buildings under the microscope: a country by country review of the energy performance of buildings, Building Performance Institute Europe, Brussels, Belgium. [Available from

http://www.bpie.eu/eu_buildings_under_microscope.html .VRFQFfmsX4I, accessed 24th March 2015]. ISBN: 9789491143014.

Brandl, H. (2006) Energy foundations and other thermo active ground structures, *Geotechnique*, 56 (2), 81 – 122.

Brettmann, T. P. E., Amis, T. & Kapps, M., 2010. Thermal conductivity analysis of geothermal energy piles, Proceedings of the Geotechnical Challenges in Urban Regeneration Conference, London, UK, 26 – 28 May 2010.

Brown, D. A., 2005. Practical Considerations in the Selection and Use of Continuous Flight Auger and Drilled Displacement Piles. ASCE Geotechnical special publication, (129), pp. 251-261.

Bozis, D., Papakostas, K., & Kyriakis, N. (2011) On the evaluation of design parameters effects on the heat transfer efficiency of energy piles, *Energy and Buildings*, 43 (4), 1020-1029.

Cecinato, F. & Loveridge, F. A. (2015) Influences on the thermal efficiency of energy piles, *Energy*, doi:10.1016/j.energy.2015.02.001.

Choi, J.C., Lee, S.R. and Lee, D.S. (2011) Numerical simulation of vertical ground heat exchangers: Intermittent operation in unsaturated soil conditions, Computers and Geotechnics, 38, 949-958.

Council Directive 2009/28/EC of 23rd April 2009 on the promotion of the use of energy from renewable sources and amending and subsequently repealing Directives 2001/77/EC and 2003/30/EC.

Gao, J., Zhang, X., Liu, J., Li, K. & Yang, J. (2008) Thermal performance and ground temperature of vertical pile foundation heat exchangers: a case study, *Applied Thermal Engineering*, 28, 2295-2304.

Hellstrom, G., 1991. Ground Heat Storage, Thermal Analysis of Duct Storage Systems, Theory. Department of Mathematical Physics, University of Lund, Sweden.

Lamarche, L., Kajl, S. & Beauchamp, B. 2010. A review of methods to evaluate borehole thermal resistance in geothermal heat pump systems, *Geothermics*, 39, 187-200.

Laloui, L., & Di Donna, A. (2012) Understanding the behaviour of energy geo-structures, *Proceedings of the Institution of Civil Engineers Civil Engineering*, 165 (1), p14.

Loveridge, F. & Powrie, W. (2013a) Performance of Piled Foundations Used as Heat Exchangers, 18th International Conference for Soil Mechanics and Geotechnical Engineering, Paris, France, September 2-5, 2013.

Loveridge, F. & Powrie, W. (2013b) Pile heat exchangers: thermal behaviour and interactions, *Proceedings of the Institution of Civil Engineers Geotechnical Engineering*, 166 (2), 178 - 196.

Loveridge, F. & Powrie, W. (2014) On the thermal resistance of pile heat exchangers, *Geothermics*, 50, 122 – 135.

Muraya, N. K., O'Neal, D. L. & Heffington, W. M. (1996) Thermal interference of adjacent legs in a vertical U-tube heat exchanger for a ground coupled heat pump, *ASHRAE Transactions*, 102 (2), 12-21.

Neville, A. M. (1995) Properties of concrete, Fourth Edition, Longman.

Ozudogru TY, Olgun CG and Senol A (2014) 3D numerical modeling of vertical geothermal heat exchangers. *Geothermics,* 51, 312–324

Rees SJ and He M (2013) A three-dimensional numerical model of borehole heat exchanger heat transfer and fluid flow. *Geothermics,* 46, 1–13

Signorelli S, Bassetti S, Pahud D and Kohl T (2007) Numerical evaluation of thermal response tests. *Geothermics,* 36, 141-166

Wood, C. J., Liu, H. & Riffat, S. B. (2010) An investigation of the heat pump performance and ground temperature of a pile foundation heat exchanger system for a residential building, *Energy*, 35, 3932-4940.

Figures

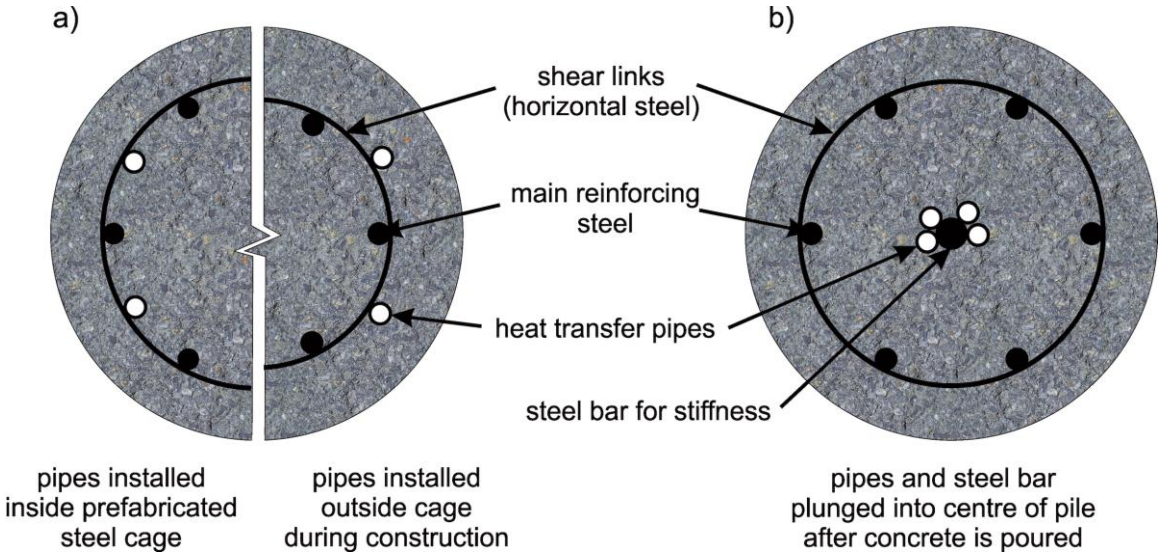

Figure 1 Typical cross sections for a) rotary bored and b) continuous flight auger piles (after Loveridge & Powrie, 2013)

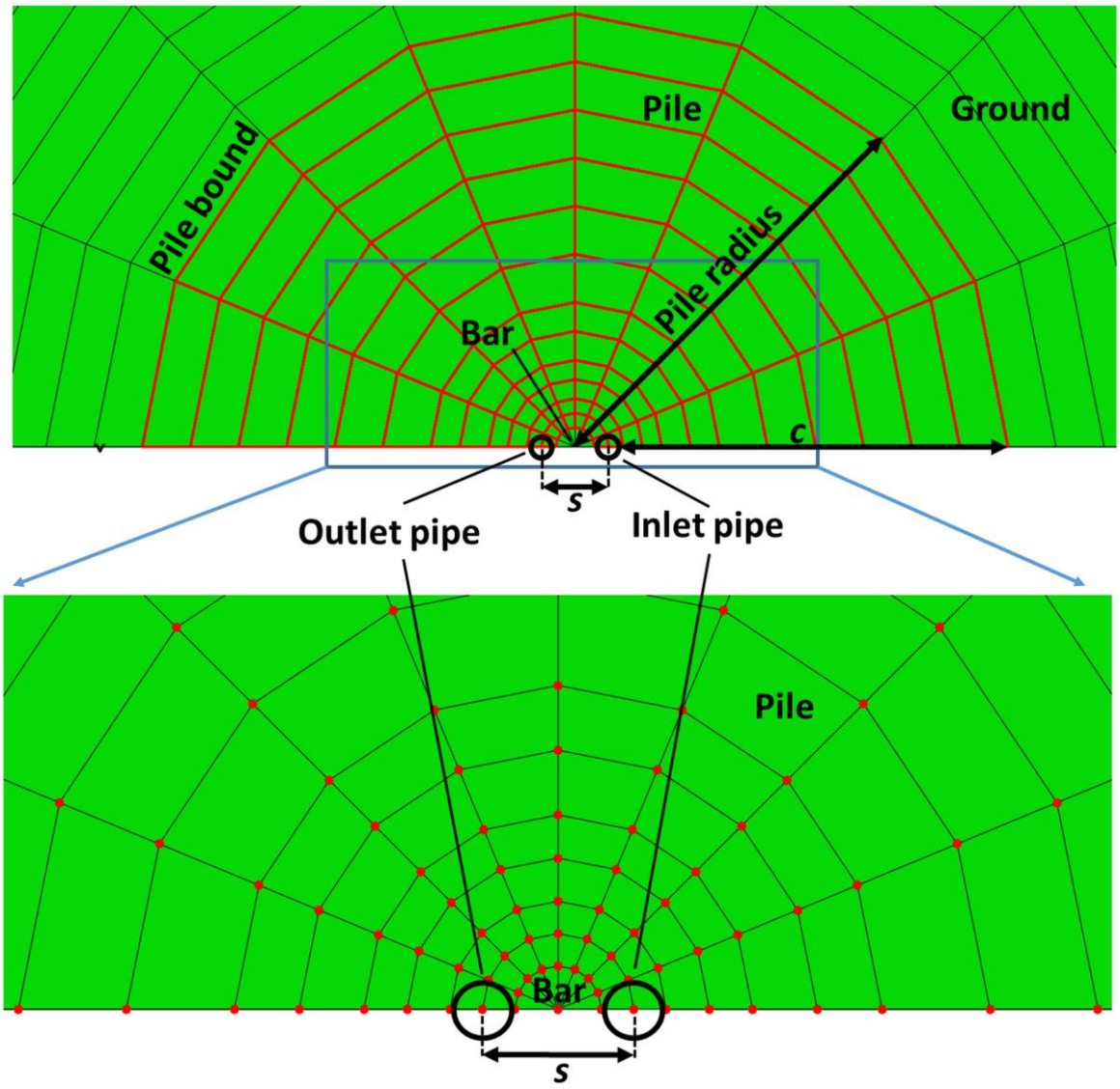

Figure 2 FE mesh for a two pipe (single U-loop) thermo-active CFA pile, with indication of the main geometrical quantities (concrete cover c=400 mm). Only half of the domain is considered in this case, for symmetry reasons. (a) Overview of the pile area (horizontal dimension= 1.15 m), (b) enlargement of bar and pipes area (horizontal dimension= 0.5 m).

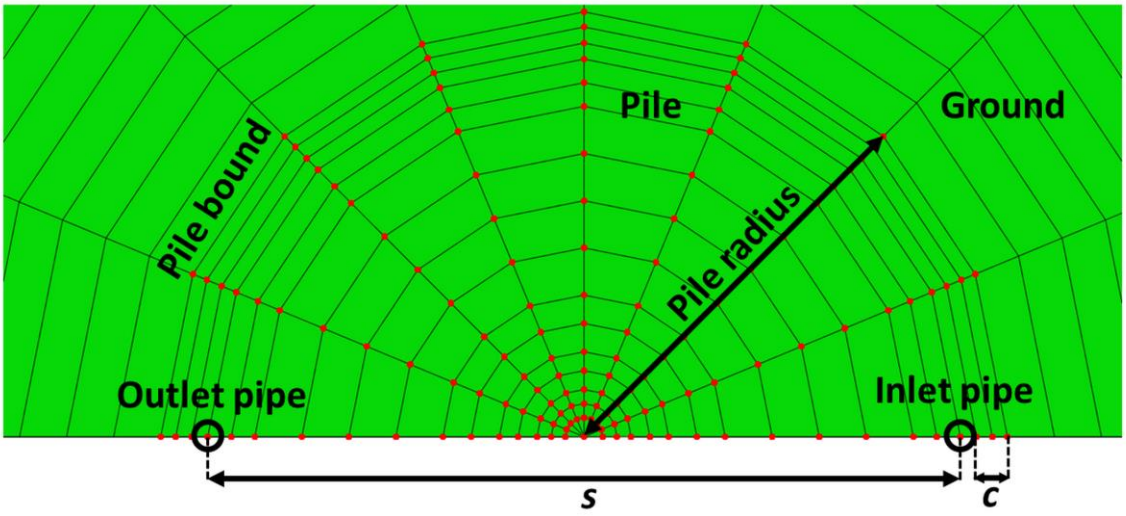

Figure 3 FE mesh for a two pipe (single U-loop) thermo-active rotary bored pile for comparison with the CFA case, with an indication of the main geometrical quantities (concrete cover c=75 mm, pipe shank spacing s=720 mm). Only half of the domain is considered in this case, for symmetry reasons (horizontal dimension= 1.2 m).

Figure 4 Unsymmetrical pipes arrangements in CFA Piles: a) a practical example of a 600 mm pile (pipes protected in pile break-out zone); b) FE mesh for simulation of this type of pipe arrangement.

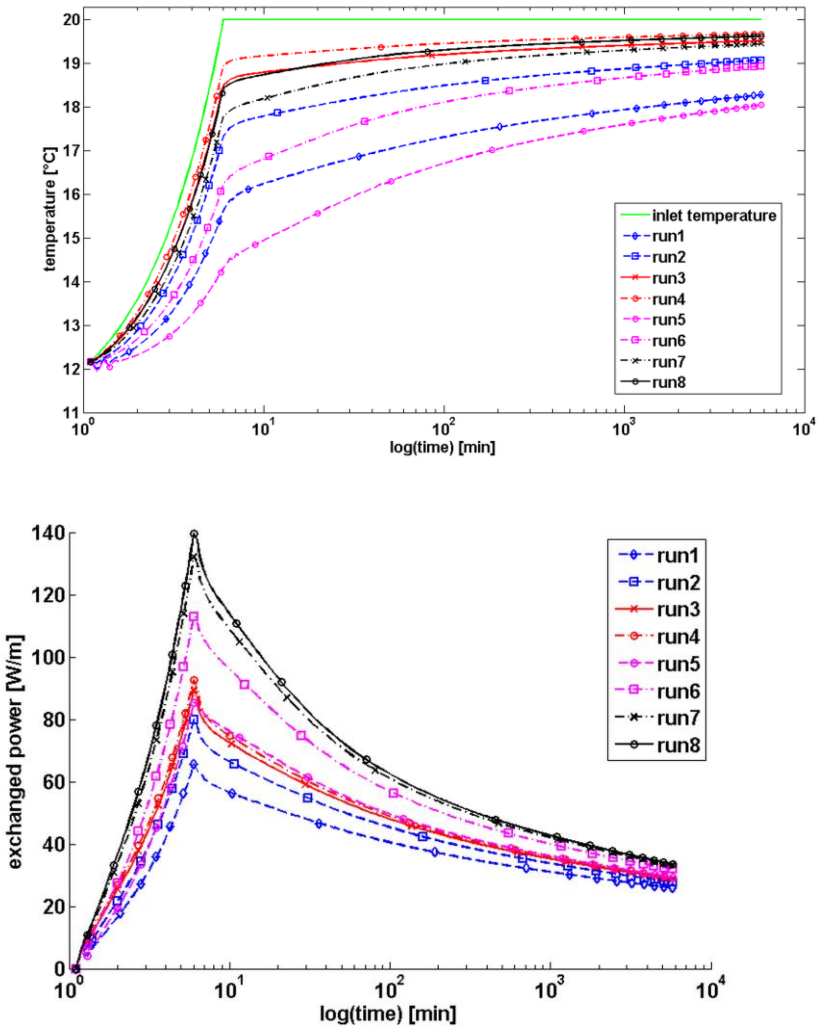

Figure 5 Results of the thermo-active CFA pile sensitivity analysis: a) fluid outlet temperature evolution; b) evolution of exchanged power per unit length.

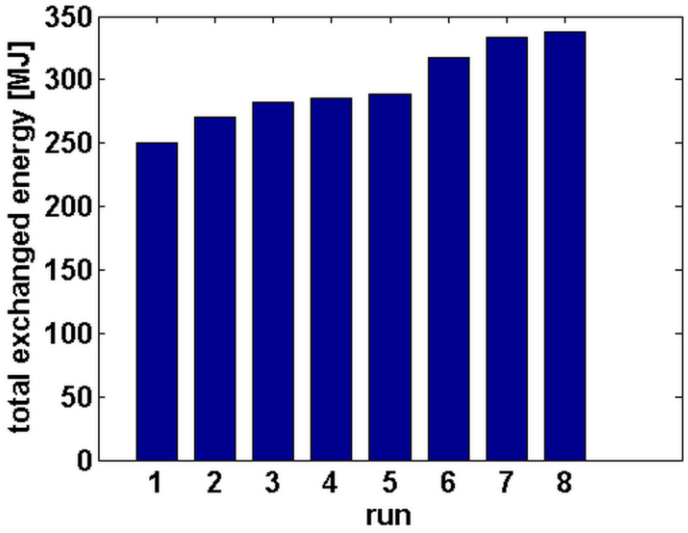

Figure 6 Results of the thermo-active CFA pile sensitivity analysis: total energy exchange for the different simulation runs.

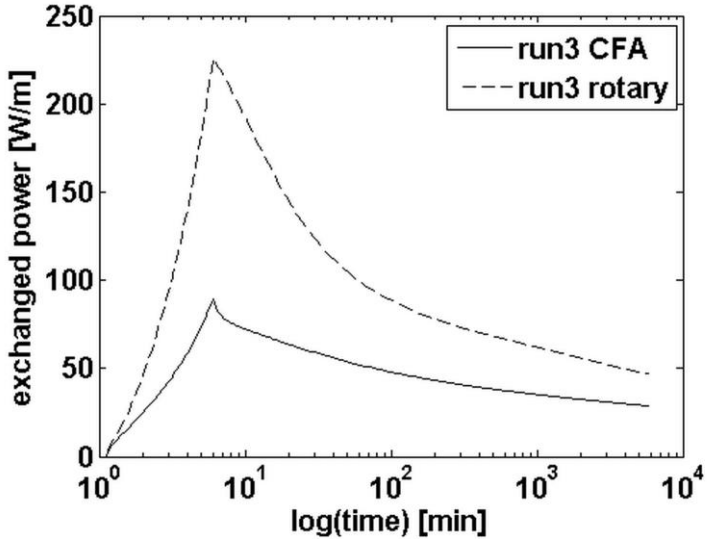
run3 CFA
run3 rotary
exchanged power [W/m]
log(time) [min]
0
50
100
150
200
250
10^0
10^1
10^2
10^3
10^4

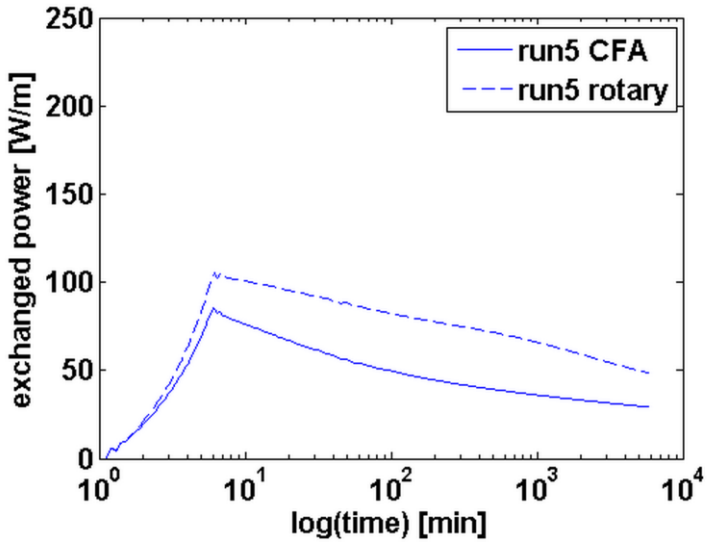
run5 CFA
run5 rotary
exchanged power [W/m]
log(time) [min]
0
50
100
150
200
250
10^0
10^1
10^2
10^3
10^4

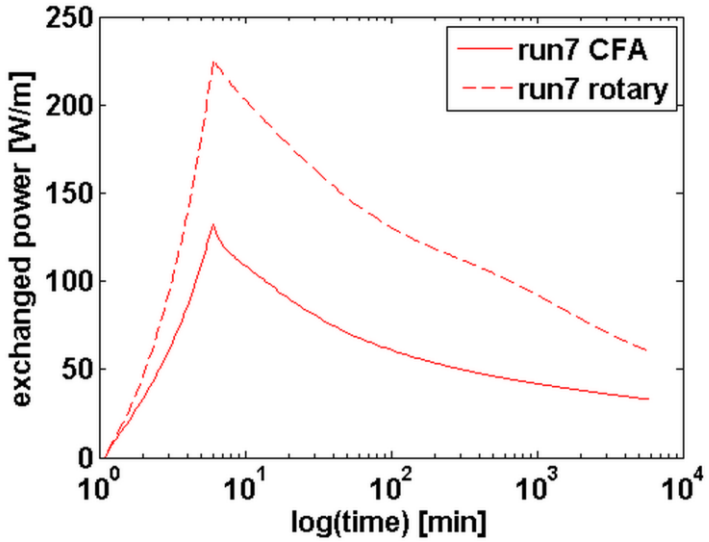
run7 CFA
run7 rotary
exchanged power [W/m]
log(time) [min]
0
50
100
150
200
250
10^0
10^1
10^2
10^3
10^4

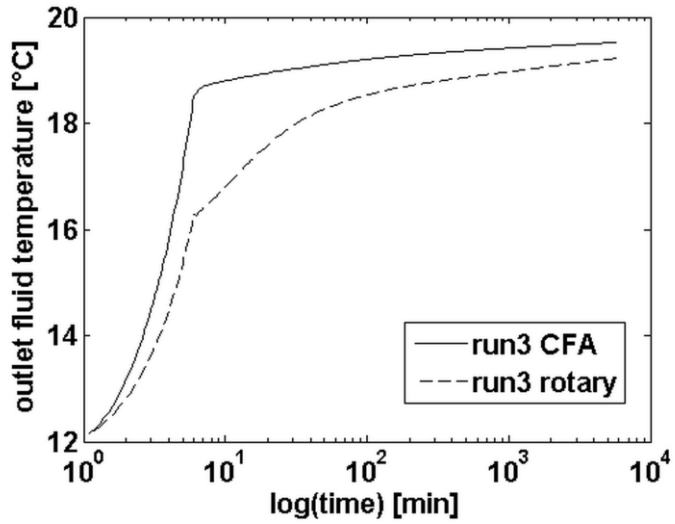

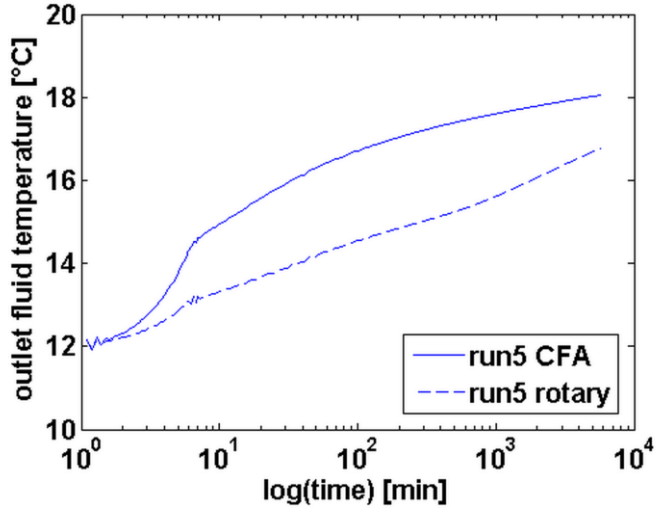

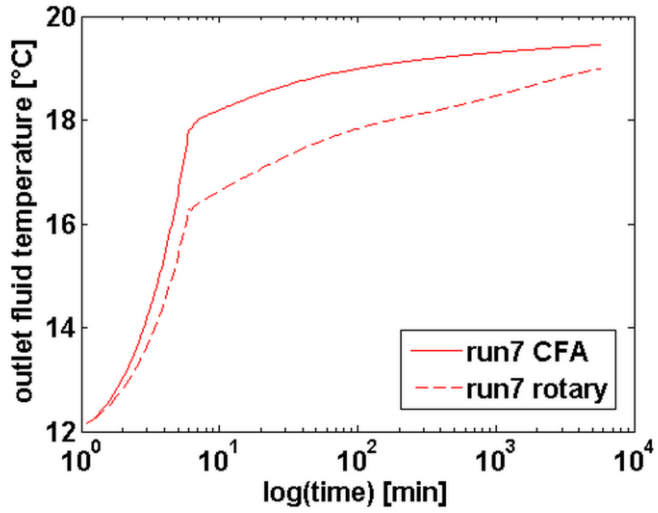

Figure 7 Comparison of thermo-active CFA piles with rotary piles: a)-c) exchanged power evolution; d)-f) fluid outlet temperature evolution.

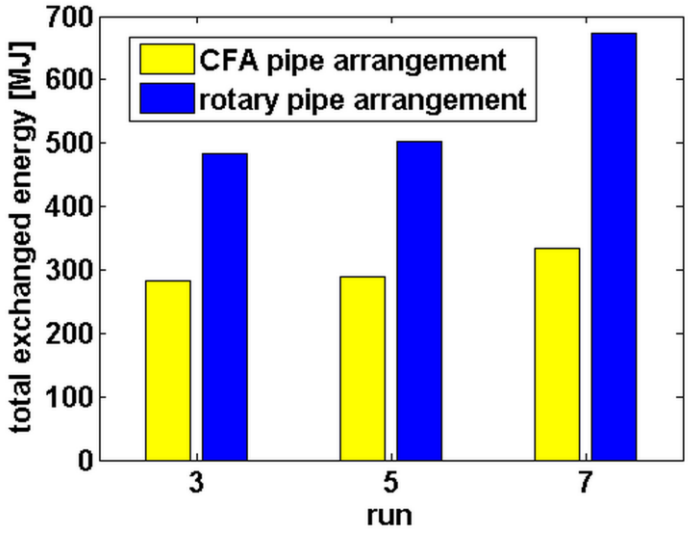

Figure 8 Comparison of thermo-active CFA pile with rotary piles: total energy exchange for the different simulation runs.

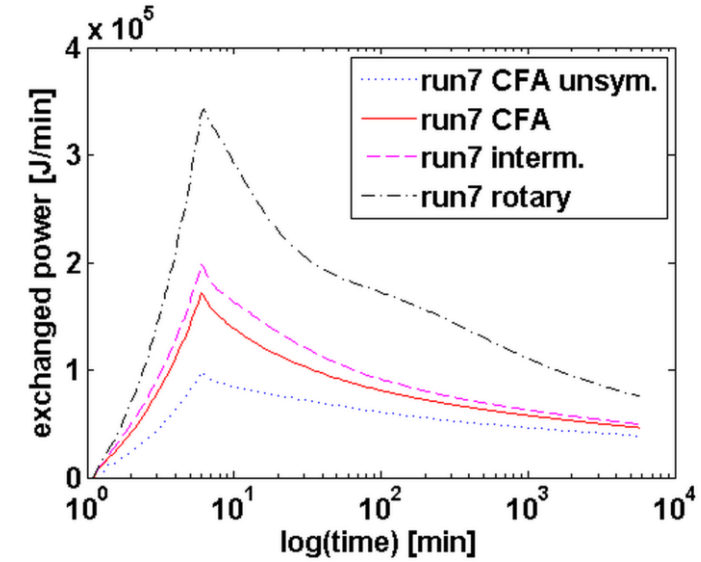

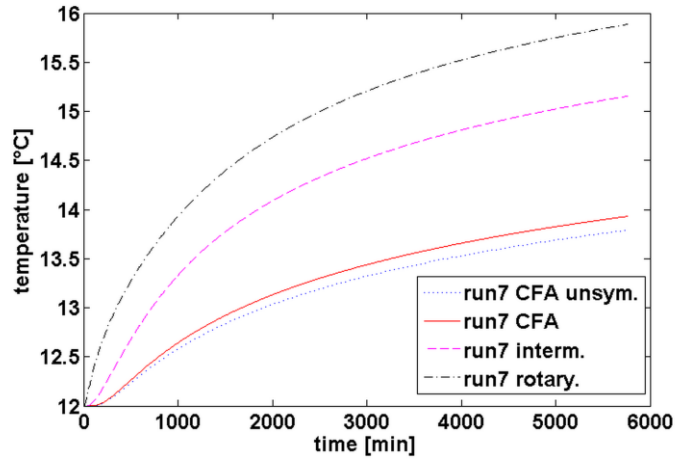

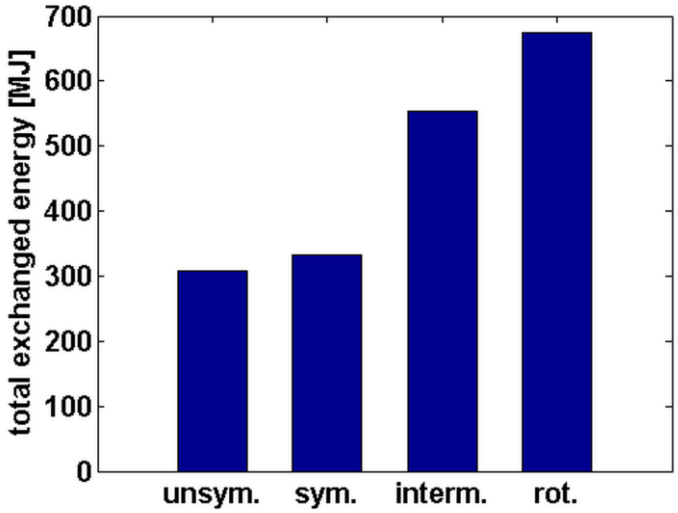

Figure 9 Comparison of different pipe arrangements in terms of (a) exchanged power evolution, (b) average pile wall temperature evolution and (c) total exchanged energy for run7, including unsymmetrical CFA and intermediate pipe arrangements.

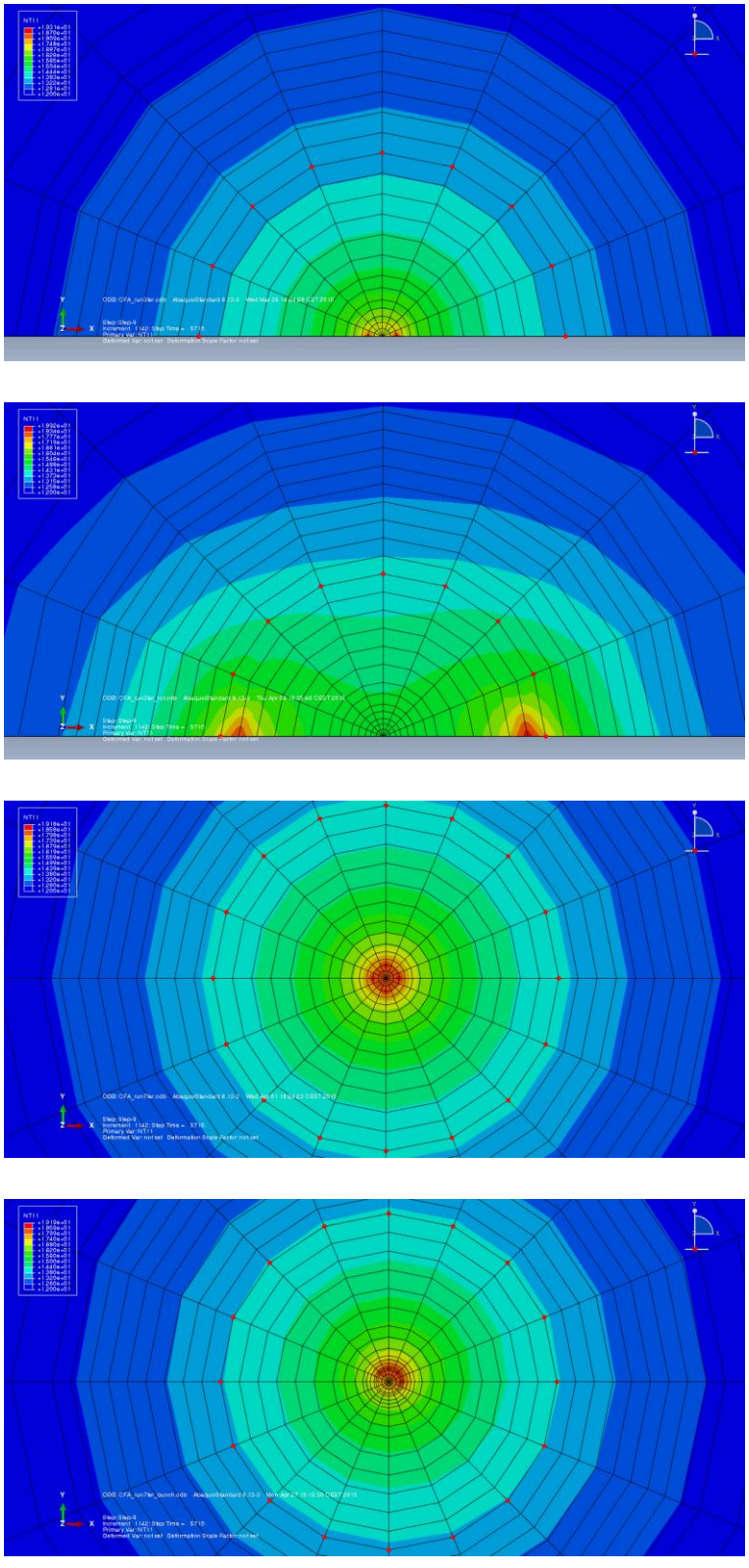

Figure 10 Temperature contours at the end of simulation (t=4 days) in a pile cross-section at mid-height (z=12.5 m) for a 2-pipe arrangement (run 3) in both CFA (a) and rotary (b) configuration, and for a 4-pipe arrangement (run7) in both symmetrical CFA (c) and unsymmetrical CFA (d) configuration.

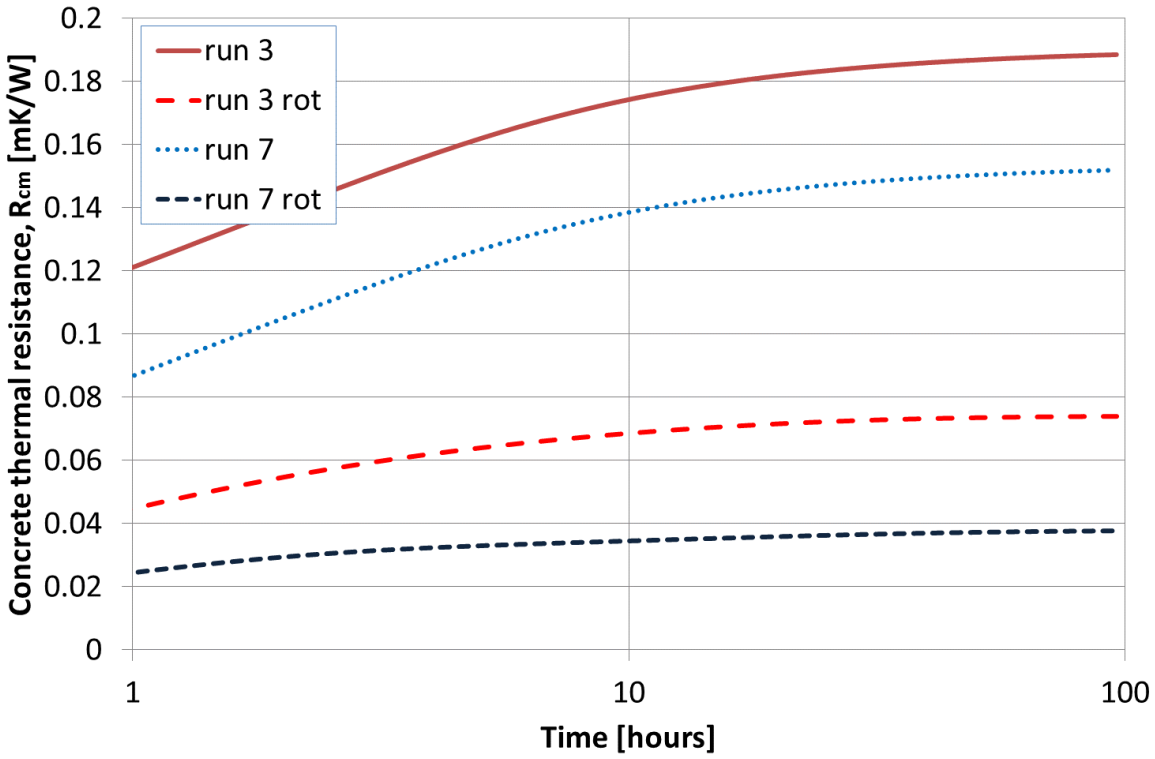

Figure 11 Example evolution of the thermal resistance with time for CFA and rotary piles containing single and double U-loops.

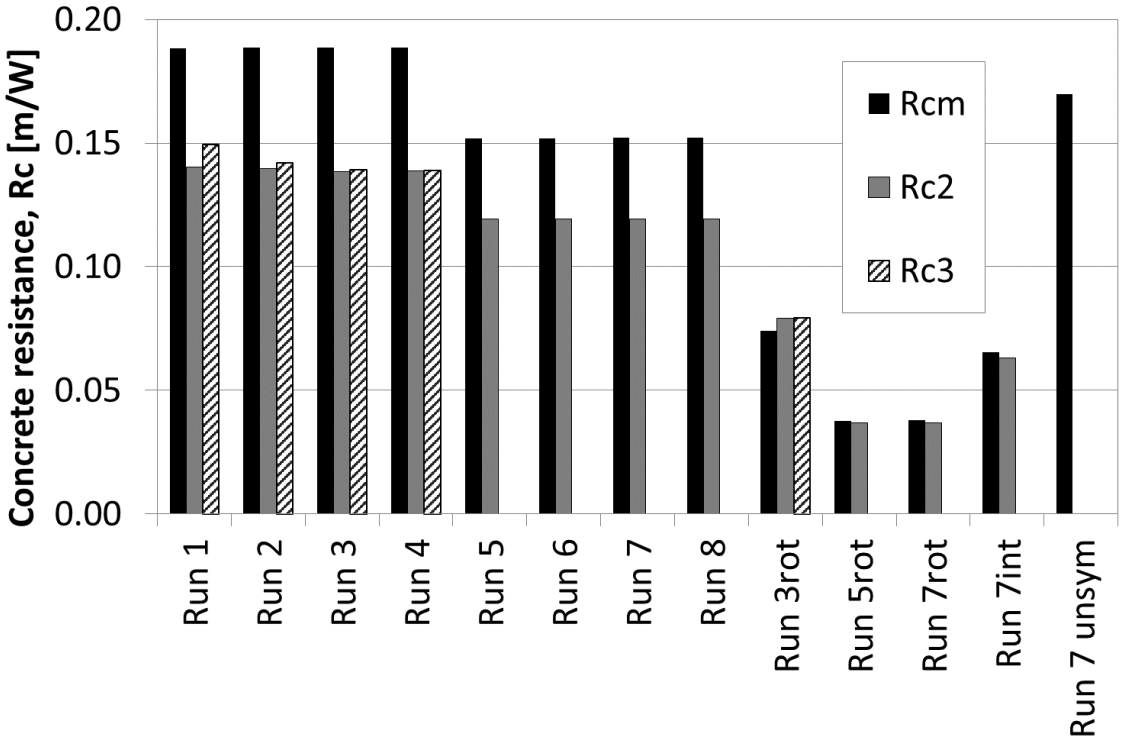

Figure 12 Comparison of numerical and analytical pile steady state concrete resistance, Rc

Tables

Table 1. Variable parameter sensitivity settings for investigation of the energy efficiency of thermo-active CFA piles. Refer to Table 2 for constant parameter settings.

	run							
Variable parameters	1	2	3	4	5	6	7	8
fluid velocity, *v* [m/s]	0.2	0.4	0.8	1.2	0.2	0.4	0.8	1.2
number of pipes, n_p	2	2	2	2	4	4	4	4

Table 2. Constant parameter values adopted in the CFA sensitivity analysis. Refer to Table 1 for variable parameter sensitivity settings.

Parameters	Value	Units
Pile diameter	900	mm
Pile length	25	m
Central bar diameter	40	mm
Pipe external diameter	30	mm
Pipe wall thickness	2.7	mm
Soil thermal Conductivity	2	W/mK
Initial soil temperature	12	°C
Ground specific heat	1600	J/(kg K)
Concrete specific heat	1000	J/(kg K)
Steel specific heat	473	J/(kg K)
Soil density	1900	Kg/m3
Concrete density	2210	Kg/m3
Steel density	7801	Kg/m3
Soil conductivity	2	W/mK
Concrete conductivity	3	W/mK
Steel conductivity	43	W/mK

Table 3. Variable parameter settings for additional simulations. Refer to Table 2 for constant parameter settings.

	run						
Variable parameters	3rot	3_Lc	3_Lh	5rot	7rot	7int	7_unsym
fluid velocity [m/s]	0.8	0.8	0.8	0.2	0.8	0.8	0.8
number of pipes	2	2	2	4	4	4	4
Pipe positions	rotary	CFA	CFA	rotary	rotary	intermediate	CFA, bunched
Shank spacing, s, [m]	0.72	0.07	0.07	0.72	0.72	0.37	0.03
Steel Conductivity [W/mK]	43	3	73	43	43	43	43